

Article

Not peer-reviewed version

Ammonia and Humidity Sensing by Phthalocyanine-Corrole complex Heterojunction Devices

[Lorena Di Zazzo](#) , Sujithkumar Ganesh Moorthy , [Rita Meunier-Prest](#) * , [Corrado Di Natale](#) * ,
[Roberto Paolesse](#) * , [Marcel Bouvet](#) *

Posted Date: 25 May 2023

doi: 10.20944/preprints202305.1768.v1

Keywords: corrole; phthalocyanine; gas sensor; organic heterojunction; conductometric transducer; molecular material



Preprints.org is a free multidiscipline platform providing preprint service that is dedicated to making early versions of research outputs permanently available and citable. Preprints posted at Preprints.org appear in Web of Science, Crossref, Google Scholar, Scilit, Europe PMC.

Copyright: This is an open access article distributed under the Creative Commons Attribution License which permits unrestricted use, distribution, and reproduction in any medium, provided the original work is properly cited.

Article

Ammonia and Humidity Sensing by Phthalocyanine-Corrole Complex Heterojunction Devices

Lorena Di Zazzo ^{1,2}, Sujithkumar Ganesh Moorthy ¹, Rita Meunier-Prest ¹, Corrado Di Natale ^{2,*}, Roberto Paolesse ^{3,*} and Marcel Bouvet ^{1,*}

¹ Institut de Chimie Moléculaire de l'Université de Bourgogne, 9 avenue Alain Savary, Dijon 21000, France;

² Department of Electronic Engineering, University of Rome Tor Vergata, Via Politecnico 1, 00133 Roma, Italy

³ Department of Chemical Science and Technology, University of Rome Tor Vergata, Via della Ricerca Scientifica, 00133, Roma

* Correspondence: dinatale@uniroma2.it (C. D. M.); roberto.paolesse@uniroma2.it (R. P.); marcel.bouvet@u-bourgogne.fr (M.B.)

Abstract: The versatility of metal complexes of corroles raised the interest in the use of these molecules as element of chemical sensors. The tuning of the macrocycle properties by synthetic modification of the different components of the corrole ring, such as functional groups, molecular skeleton, and coordinated metal, allows the creation of a vast library of corrole-based sensors. However, the scarce conductivity of most of aggregates of corroles limits the development of simple conductometric sensors and requires the use of optical or mass transducers that are rather more cumbersome and less prone to be integrated in microelectronics systems. To compensate the scarce conductivity, corroles are often used to functionalize the surface of conductive materials such as graphene oxide, carbon nanotubes, or conductive polymers. Alternatively, they can be incorporated in heterojunction devices where they are interfaced with a conductive material such as a phthalocyanine. Herewith, we introduce two heterojunction sensors made of junctions of lutetium bisphthalocyanine (LuPc_2) with either 5,10,15-tris(pentafluorophenyl) corrolato Cu (**1**) or 5,10,15-tris(4-methoxyphenyl)corrolato Cu (**2**). Optical spectra show that after forming the heterojunction, corroles maintain their original structure. The conductivity of the devices reveals an energy barrier for interfacial charge transport, which is larger in the **1/LuPc₂** device. The different interfacial barriers is also manifested by the opposite response respect to ammonia: with a **1/LuPc₂** behaving as a n-type conductor and **2/LuPc₂** as a p-type conductor. Furthermore, the sensors show a high sensitivity respect to relative humidity with a reversible and fast response in the range 30-60%.

Keywords: corrole; phthalocyanine; molecular materials; organic heterojunction; gas sensors; conductometric transducers

1. Introduction

Among gas sensing materials, molecular materials are extensively studied because they offer lots of possibilities to tune their electrical and optical properties and the intermolecular interactions they can develop with the target species. Among molecular materials, porphyrinoids, namely phthalocyanines and porphyrins have been highly studied [1–4]. They are characterized by large π -aromatic systems and can reversibly interact with many molecules, by H-bonds, dipole-dipole and van der Waals interactions, their metal center offering coordination bonding. They offer the possibility of electron transfer with redox active species. This is the reason why they have been used in numerous applications, e.g. for air quality monitoring [5], for controlling the freshness of food [6,7] and also for the analysis of biomarkers in breath [8]. Another family of porphyrinoids has been introduced more recently in the field of chemosensors, namely corroles [9–12], which have been used

as sensing materials associated with optical, acoustic, electrochemical and conductometric transducers, as recently reviewed [13]. While porphyrins are characterized by an aromatic macrocyclic system containing 22 electrons, corroles are contracted porphyrins, with a molecular skeleton featuring that of corrin, the nucleus of Vitamin B12. Corrole was reported for the first time in the early 60s [14], but it gained renewed attention recently, after the discovery of simple synthetic routes for its preparation [15,16]. Considering conductometric sensors, because of the rather low conductivity of corroles, they are often associated with more conducting materials, e.g. carbon nanotubes [10] and reduced graphene oxide [17], both applied to the detection of nitrogen dioxide. Another way to use low conducting material in conductometric transducers is to incorporate them into heterojunctions. Thus, two types of molecular material – based heterojunction devices were recently reported, namely double layer heterojunctions [18] and double lateral heterojunctions [19]. The latter were obtained by depositing material by an electrodeposition technique, as electropolymerization. Thus, starting from 2,3,5,6-tetrafluoroaniline, we deposited the perfluoropolyaniline [19] and from the zinc porphine we deposited the corresponding polyporphine [20]. Very recently, we reported the first example of electrodeposited polycorrole, starting from 5,10,15-(4-aminophenyl)corrolato]copper(III) as monomer [21]. In the case of double layer heterojunctions, the deposition technique can be the evaporation under vacuum [22,23] or any solution processing technique [24]. The common point of these heterojunction devices is that the top layer is made of a more conducting material (Figure 1).

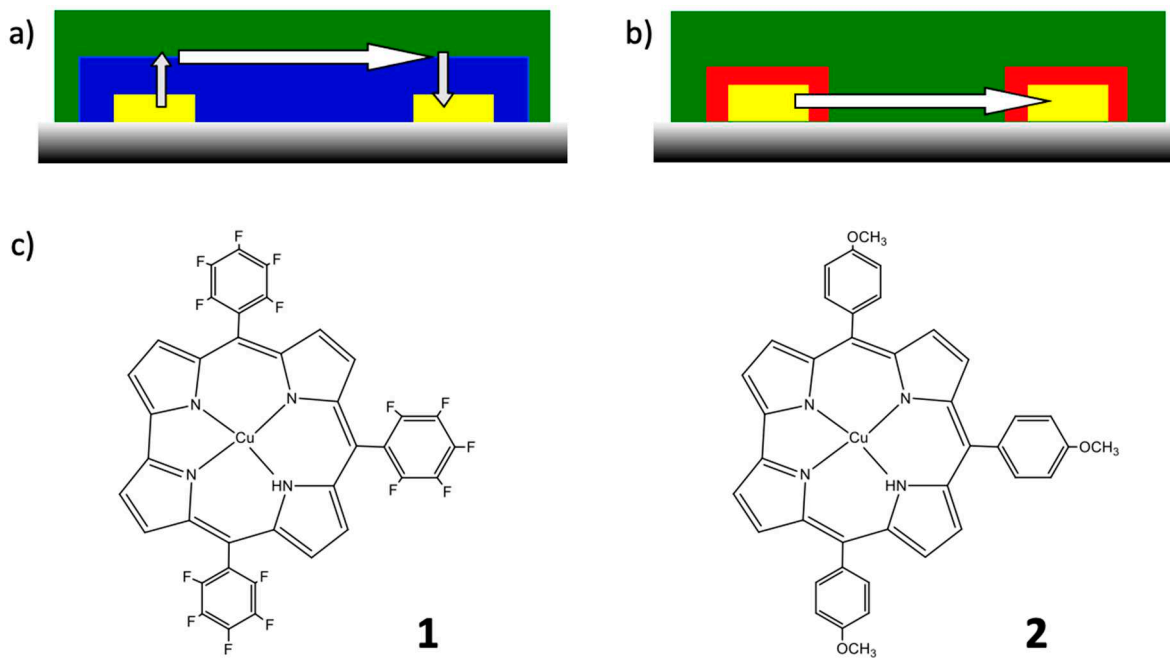


Figure 1. Scheme of double layer heterojunction (a) and double lateral heterojunction (b) devices. The arrows indicate the main path for charges flowing from one electrode to the other one. (c) View of 5,10,15-tris(pentafluorophenyl) corrolato Cu (**1**) and 5,10,15-tris(4-methoxyphenyl) corrolato Cu (**2**) complexes.

In the present work, we report the use of Cu (III)-tris(pentafluorophenyl) corrole (CuTpFPC, **1**) and Cu (III)-tris(p-methoxyphenyl) corrole (Cu-(pmethoxy) TPC, **2**) as sublayers in molecular materials – based double layer heterojunction devices (Figure 1a), combining them with a highly conducting molecular material, namely the lutetium bisphthalocyanine, LuPc₂. Due to its radical nature, LuPc₂ exhibits a high conductivity at room temperature and can be easily oxidized and reduced [25], which make such a sensor highly sensitive to redox active species [2]. However, the

transport properties of these heterojunction devices are determined by the nature of charge carriers in the sublayer, which can be p-type, n-type or ambipolar [26].

2. Experimental section

2.1. Chemicals and syntheses

Lutetium bisphthalocyanine (LuPc_2) was synthesized according to the literature [27]. Dichloromethane was procured from a local supplier and was distilled before use in solutions preparation. Tetrabutylammonium perchlorate (> 98%) (TBAP) and copper acetate (Cu(OAc)_2) were purchased from Sigma-Aldrich. Thin-layer chromatography (TLC) was performed on Sigma-Aldrich silica gel plates. Chromatographic purification of the reaction products was accomplished by using silica gel 60 (70–230 mesh, Sigma-Aldrich, St. Louis, MO, USA) as a stationary phase. Corrole free bases were synthesized according to literature [28].

Cu (III)-tris (pentafluorophenyl) corrole (1): 95.3 mg of tris (pentafluorophenyl) corrole (1.2×10^{-4} mol) were dissolved in 187 mL of CHCl_3 , a few drops of a saturated solution of Cu(OAc)_2 in CH_3OH were added and the mixture was stirred to reflux for 45 min. The course of the reaction was monitored by UV-vis spectroscopy and TLC (silica gel, CH_2Cl_2). After 20 min, there was no evidence of the starting material, and the solvent was removed under vacuum. The crude product was dissolved in CH_2Cl_2 and purified by column chromatography (silica gel), with CH_2Cl_2 as eluent. A brown fraction corresponding to **1** was obtained as the major product (69.6 mg, 73 % yield).

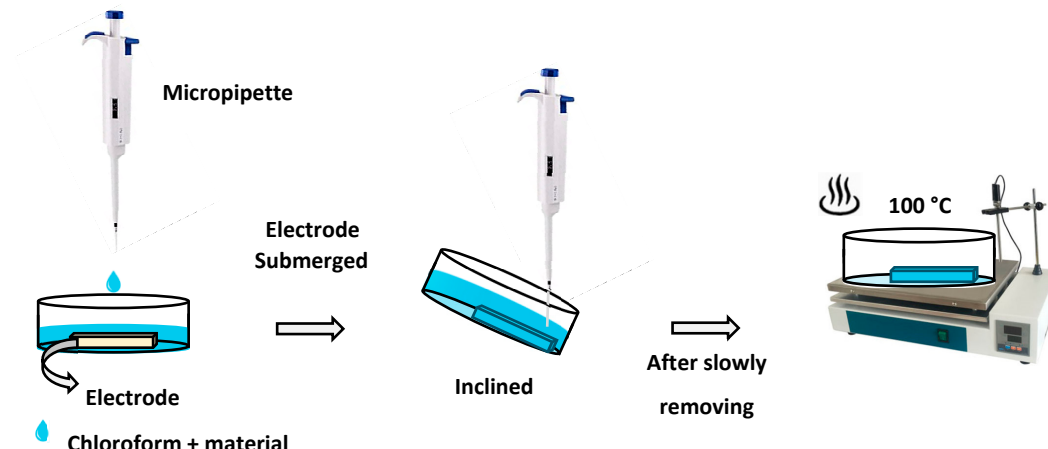
Cu (III)-tris(p-methoxyphenyl) corrole (2): Tris-(p-methoxy)phenylcorrole (98 mg, 1.6×10^{-4} mol) were dissolved in 192 mL of CHCl_3 and a saturated solution of Cu(OAc)_2 in CH_3OH was added. The progress of the reaction was monitored by UV/vis spectroscopy and TLC analysis (silica, CH_2Cl_2). After the disappearance of the starting material, the solvent was removed under reduced pressure and the residue was purified by column chromatography (silica gel, CH_2Cl_2), with **2** as the major product (77 mg, 79 % yield).

2.2. Cyclic voltammetry

Electrochemical experiments were performed at PGSTAT302N Autolab Metrohm potentiostat interfaced with Nova 2.1 software. Cyclic voltammetry was carried out on a three-electrode setup consisting of a glassy carbon disk (3 mm in diameter) as working electrode, a platinum wire as a counter electrode, and an Ag/AgCl (NaCl 3 M) as a reference, called hereafter Ag/AgCl , isolated from the solution by a salt bridge containing the same electrolyte solution as in the cell to prevent any leakage of NaCl into the cell ($E_{\text{Ag}/\text{AgCl}} = -0.066$ V vs. SCE). The working C disk electrode was soaked for 10 min in KOH (2 M), polished with 0.1 μm alumina, etched for 10 min in concentrated sulfuric acid (2 M) and sonicated 10 min in water, and then in absolute ethyl alcohol. The cyclic voltammograms were performed in CH_2Cl_2 containing 0.1 M tetrabutylammonium perchlorate, TBAP, as supporting electrolyte. The solutions were deoxygenated for 10 min with argon, and a positive overpressure of argon was maintained above the electrolyte during the entire measurement performed at room temperature.

2.3. Samples preparation

ITO Interdigitated electrodes (IDE) deposited onto $1 \times 1 \text{ cm}^2$ float glass substrate and separated by 75 μm with 50 nm thickness were sonicated three times with CH_2Cl_2 and ethanol, for 5 minutes at each step and dried in an oven for 1 hour at 100 °C. Corroles were deposited on ITO substrates with a new type of deposition method called quasi-dip coating method that we developed (Scheme 1), starting from 10^{-4} M CHCl_3 solutions of **1** or **2**. This method is quite different from the classical dip coating, since here the solution was poured into the Petri dish, which contains target substrate, till the substrate was submerged in solution, then the solution was sucked out slowly by slightly tilting the Petri dish up to 45° and dried at 100 °C. In this way, we obtained highly homogeneous surface for these materials compared to classical solvent casting technique.



Scheme 1. Schematic view of the quasi-dip coating method used for the sublayer deposition.

The corrole complex modified IDE was then transferred into a UNIVEX 250 thermal evaporator (Oerlikon, Germany) and LuPc₂ was deposited as the top layer (50 nm in thickness as controlled by a quartz crystal microbalance) through classical thermal evaporation under secondary vacuum, at *ca.* 1.0×10^{-6} mbar, and a sublimation temperature *ca.* 410-420 °C.

2.4. Spectroscopic characterization of devices

The UV-Vis spectra of the heterojunctions coated on a glass plate were recorded on a Varian's Cary® 50 spectrophotometer, using Xenon flash lamp as an excitation source, in the range of 300-900 nm. The spectra of corrole complexes in CHCl₃ solution were also recorded in the same range using a 10 mm quartz cuvette. Raman spectra of the devices and corrole powders were acquired by using a Renishaw inVia Raman microscope, using a 473 nm laser as an excitation source.

2.5. Electrical and gas sensing measurements

The fundamental electrical and sensor measurements were performed using a Keithley 6517b electrometer with an incorporated DC voltage supply, always at room temperature (19-21°C). The electrometer was controlled by a self-made software via the GP-IB board. Current-voltage (I-V) curves were registered in the range -10 – +10 V, starting and finishing at 0 V bias to avoid irreversible polarization effects [29]. Ammonia gas, at 985 and 98 ppm in synthetic air, and synthetic air were used from standard gas cylinders, purchased from Air Liquide, France.

NH₃ sensing experiments were performed dynamically through alternative exposure to different ammonia concentrations in the range 1 – 90 ppm, for either 1 min or 10 min and recovery cycle under clean air for either 4 or 40 min, respectively, at controlled relative humidity (RH). The required humidity in the chamber was produced through a humidity generator connected with the fluidic line and controlled in the range 30%-60% by a commercial humidity sensor (HMT-100, Vaisala, Finland). The system is semiautomated, in which the opening of the mass flow controller valves, mixing of the gases, control of relative humidity (RH) and data acquisition were operated by a customized software.

3. Results and discussion

3.1. Syntheses

The Cu complexes have been obtained by synthetic methods adapted from literature [28]. The electronic absorption spectra clearly show the successful metalation (Figure S1). Thus, the Soret bands are modified, with a shift from 417 to 433 nm for the copper complex **2**. The number of Q bands is decreased from metal free corroles to copper complexes due to the change in symmetry.

3.2. Electrochemical characterization

The cyclic voltammograms of corroles **1** and **2** (Figure 2) present two redox systems: one reduction step at $E_1^{Red} = -0.13V$ vs. $Ag/AgCl$ and $E_2^{Red} = -0.635V$ vs. $Ag/AgCl$, respectively and one oxidation step at $E_1^{Ox} = 0.83V$ vs. $Ag/AgCl$ and $E_2^{Ox} = 0.285V$ vs. $Ag/AgCl$, respectively. It must be mentioned that substituents on the phenyl groups in meso position have a strong influence on the potential position. Thus, when the three meso groups are (p-methoxy)phenyls, the potentials of the reduction and oxidation peaks are shifted by more than 500 mV in the negative direction compared to those obtained for corrole **1**, substituted by three pentafluorophenyl groups. These peaks are associated with the reduction and oxidation of the macrocyclic ring and can be used to estimate the energy values of the HOMOs and LUMOs frontier orbitals. Therefore, the onset values (Figure 2) versus SCE as reference electrode were reported in eqs. (1) and (2) [30].

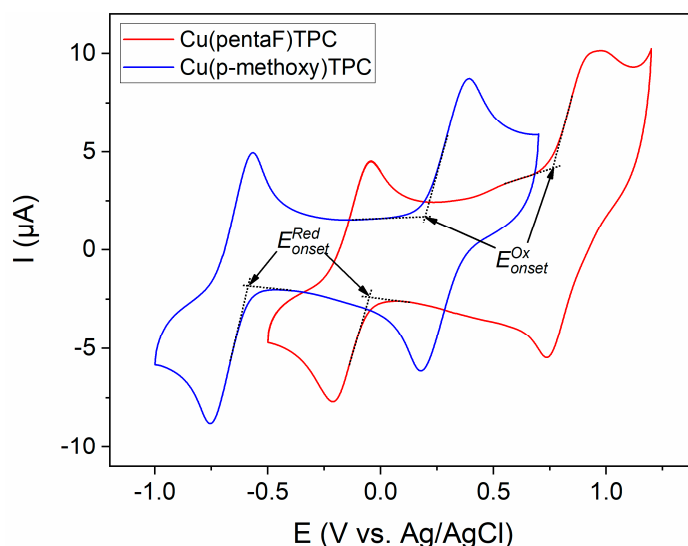


Figure 2. Cyclic voltammograms of 10^{-3} M of **1** (red) and **2** (blue), on glassy carbon electrode, in CH_2Cl_2 + 0.1 M TBAP, at a scan rate of 0.1 Vs^{-1} .

$$E_{HOMO} = -(E_{onset}^{Ox} + 4.4) \quad (1)$$

$$E_{LUMO} = -(E_{onset}^{Red} + 4.4) \quad (2)$$

The energies of the HOMO and LUMO of **1** are -4.90 and -4.28 eV, respectively, and -4.55 and -3.75 eV, respectively, for **2**.

3.3. Device characterization

Devices were obtained by successive deposition of a corrole complex by the solution processing technique above described, followed by vacuum evaporation of a 50 nm – thick LuPc₂ layer.

3.3.1. Spectroscopic characterization

The optical absorption spectra of corrole complexes **1** and **2** deposited on glass with the quasi-dip coating technique highlight a good deposition with a good molecular dispersion on the substrate. The two different corroles show good adhesion and coverage on the plain glass. Compared to the $CHCl_3$ solutions, the spectra are slightly broadened, with a red shift of the Soret and Q bands, by 7 nm for both bands of **1** at 410 and 560 nm, by 9 nm for the Soret band of **2** at 441 nm and by 10 and 20 nm for its two Q bands, at 551 and 647 nm, which are actually shoulders (Figure 3). These red shifts indicate the formation of J aggregates associated with edge-to-edge intermolecular interactions in the solid state [31].

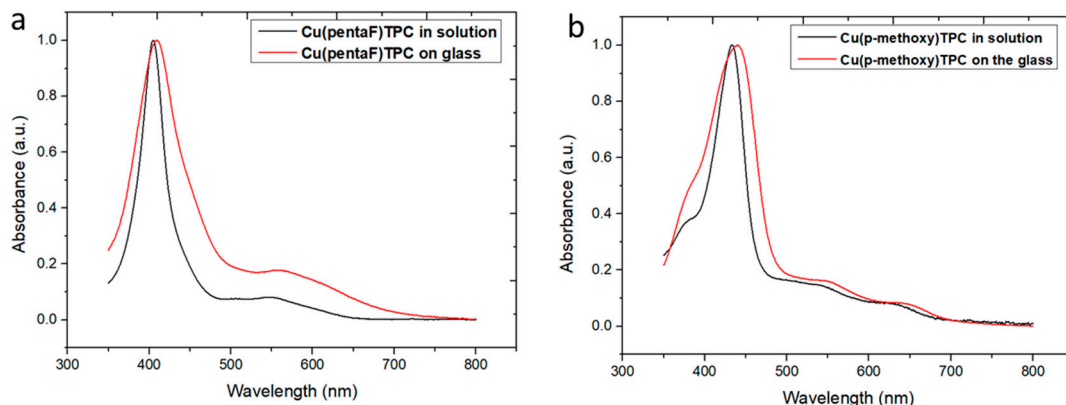


Figure 3. UV-visible electronic absorption spectra of **1** (a) and **2** (b) in CHCl_3 solution (black) and on glass (red).

The bilayer heterojunction devices **1/LuPc₂** and **2/LuPc₂** were obtained by coating films of **1** and **2** by thermal evaporation a LuPc₂ top layer. The formation of heterojunctions was confirmed by measuring the optical absorption spectra (Table 1). Both heterojunctions exhibit the same peak at 669 nm, which belongs to LuPc₂ and corresponds to its Q-band (Figure 4) [32]. The bands at 605 and 604 nm correspond to the so-called “blue vibration band” of LuPc₂. The peak at 460 nm that corresponds to a transition towards the semi-occupied molecular orbital of LuPc₂ appears as a shoulder at ca. 460 nm in the spectrum of **1/LuPc₂** (Figure 4a) and is masked in **2/LuPc₂** by the Soret band of **2** (Figure 4b). Indeed, the main contribution of corrole complexes appears in the range 350-500 nm (Soret bands) as broadened peaks, at 409 nm for **1** (Figure 4a) and at 439 nm for **2** (Figure 4b). So, the spectra of heterojunctions appear as the superimposition of the spectra of both layers.

Table 1. Maximum absorption wavelengths of **1** (a) and **2** (b) in CHCl_3 solution and on glass (red) compared to these of heterojunctions and of a LuPc₂ film.

Chemical	Soret band and other bands (nm)	Q band (nm)
LuPc ₂	460, 605	669
CuTpFPC (1) in solution	403	553
CuTpFPC (1) on glass	410	560
1/LuPc₂ heterojunction	409, 460, 604	669
CuTpmethoxyPC (2) in solution	432	541, 627
CuTpmethoxyPC (2) on glass	441	551, 647
2/LuPc₂ heterojunction	439, 605	669

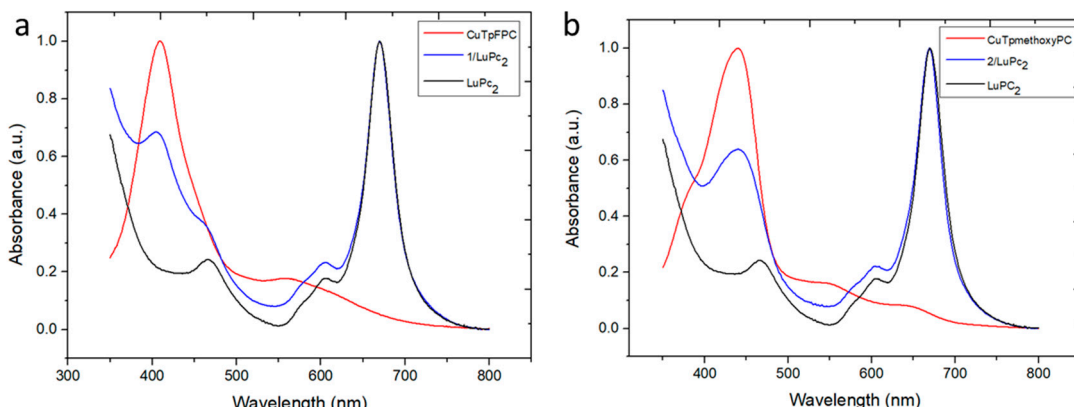


Figure 4. UV-visible absorption spectra of **1**/LuPc₂ (a) and **2**/LuPc₂ (b) heterojunction devices compared to these of films of **1** or **2** and this of a LuPc₂ film.

To get a wider chemical characterization of the heterojunction devices based on the corrole complexes and LuPc₂, they were studied by Raman spectroscopy (Table S1). Some peaks correspond to the sublayer, at 646, 1016, 1080, 1340 cm⁻¹ (C_α-C_α bonds) and an intense peak at 1529 cm⁻¹ attributed to C-F binding, while other peaks can be assigned to the top layer LuPc₂, namely 578 cm⁻¹ corresponding to Pc breathing, at 780 cm⁻¹ to C=N aza breathing, at 1408 cm⁻¹ to C_α-C_{meso} and at 1601 cm⁻¹ to C=C in the benzene ring [33]. So, the Raman spectrum of the **1**/LuPc₂ heterojunction shows peaks that can be attributed to the two layers (Figure 5).

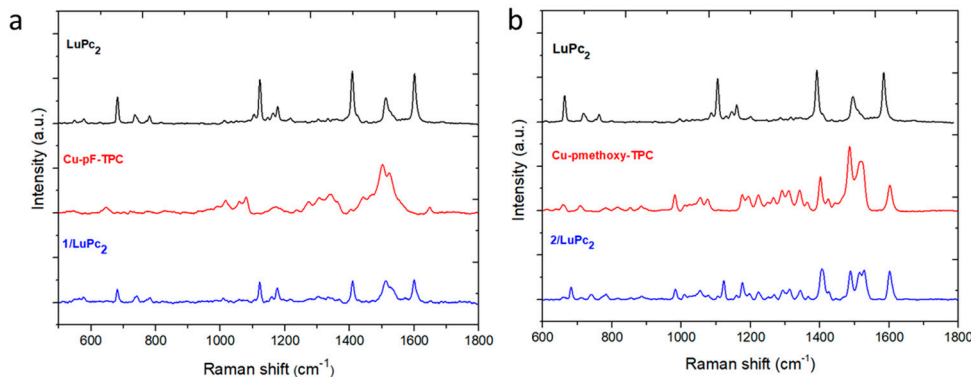


Figure 5. Raman spectra of **1**/LuPc₂ (a) and **2**/LuPc₂ (b) heterojunctions compared to these of films of **1** or **2** and this of a LuPc₂ film.

The same feature appears for **2**/LuPc₂, with some peaks that can be attributed to the sublayer at 661, 884.5, 982, 1075.5, 1196, 1292, 1312, and 1343 cm⁻¹ (C_α-C_α bonds), while the main peaks of the LuPc₂ top layer are well visible, namely 680, 1122 and 1407 cm⁻¹. Additionally, a few peaks are common to both materials, as the peaks at 735 cm⁻¹ (C-H wagging), at 780 cm⁻¹ (C=N aza stretching), at 1177 cm⁻¹ (C-H binding), and at 1221 cm⁻¹ (C-H binding) and 1601 cm⁻¹ (benzene stretching). These results also confirm that the development of heterojunctions with the two types of corrole complexes and LuPc₂ is achieved correctly without decomposing the material.

3.3.2. Electrical characterization

The electrical properties of functionalized electrodes were investigated by recording the current-voltage (I-V) curves in the range from -10 to +10 V. The **1**/LuPc₂ heterojunction device exhibits non linear I-V characteristics showing the existence of an interfacial energy barrier between the two materials. The apparent energy barrier estimated from the tangent to the I-V curve at high bias was 1.15 V, which is a rather low value (Figure 6). In the contrary, the **2**/LuPc₂ heterojunction device exhibits a linear behavior associated with ohmic contacts. The current values at 10 V of the former and the latter are of 6×10^{-6} A and 1.5×10^{-5} A, respectively. The I-V curves are symmetrical, as expected for such symmetrical devices [18].

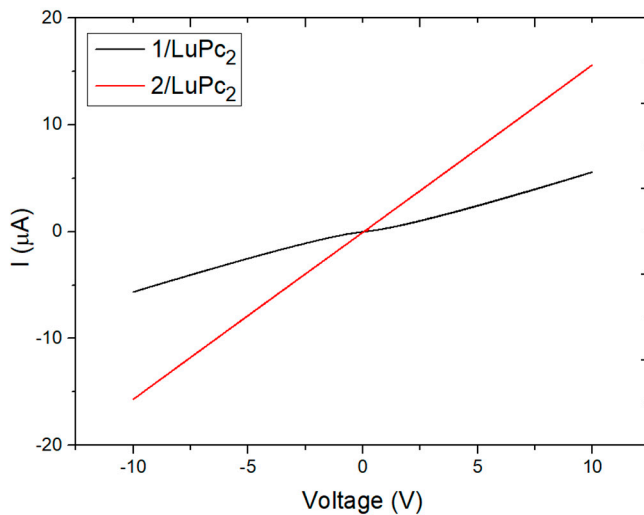


Figure 6. I-V curves of the **1/LuPc₂** (black) and **2/LuPc₂** (red) heterojunctions.

3.4. Ammonia sensing properties

The response of the devices toward ammonia were studied by submitting them to two types of exposure: long exposure (10 min) at a constant NH₃ concentration (90 ppm) and short exposure (1 min) at different NH₃ concentrations (10-90 ppm), each exposure period being followed by recovery periods of 30 min and 4 min, respectively. For **2/LuPc₂** device, current decreases under ammonia and increases under clean air (Figure 7). Considering the electron-donating nature of ammonia, the heterojunction device is of p-type, NH₃ molecules neutralizing positive majority charge carriers.

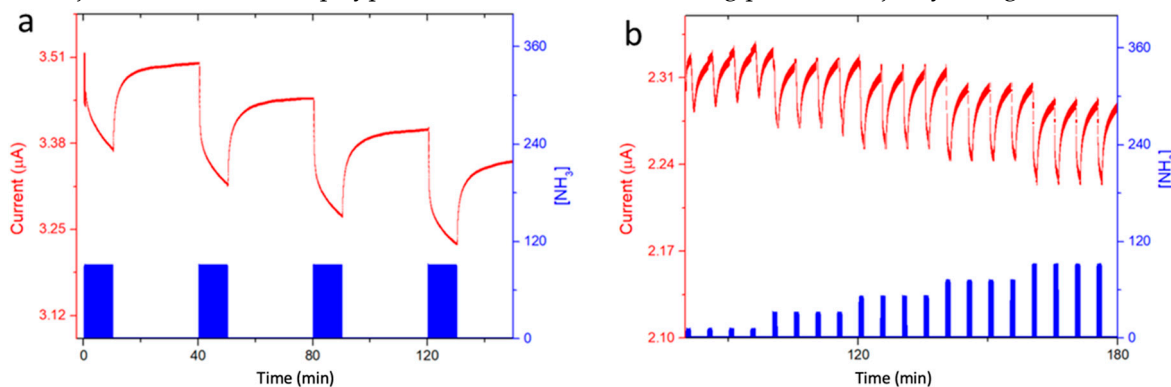


Figure 7. Current variation as a function of time for **2/LuPc₂** heterojunction device exposed to 90 ppm NH₃ for 10 min-long periods separated by 30 min-long rest periods in synthetic air (a), and in the range 10-90 ppm with 1 min/4 min exposure/recovery cycles (b), both at 40% RH and a bias of 3 V.

The absolute response ΔI defined as $I_0 - I_f$, I_0 and I_f being the current values at the beginning and at the end of an exposure period, and consequently the relative response (RR) defines as $100 \times \Delta I/I_0$, were calculated for the short exposures to NH₃ (Figure 8). The absolute values of ΔI and RR increase almost linearly with the NH₃ concentration up to 50 ppm, then saturation of sensors occurs. From the linear part, the sensitivity S , defined as the slope of the $RR = f([NH_3])$ curve, was $2.5\% \text{ ppm}^{-1}$.

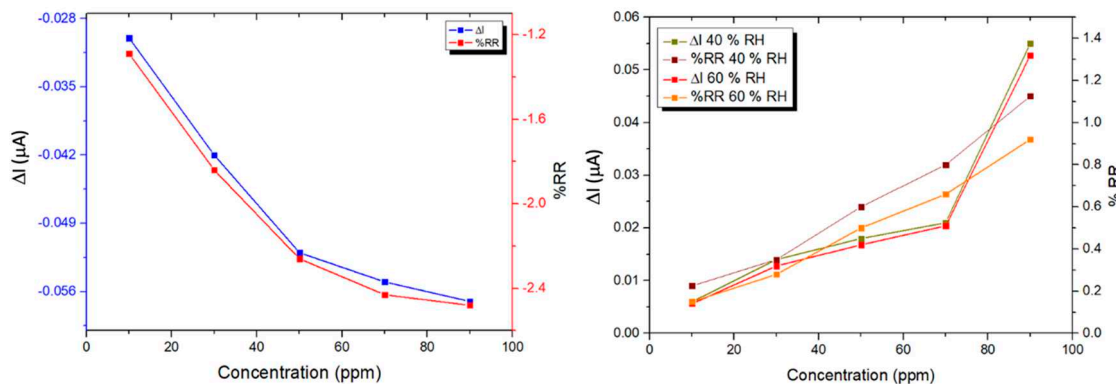


Figure 8. ΔI and RR as a function of the NH_3 concentration for **2**/LuPc₂ heterojunction devices, as depicted from Figure 7 (left) and RR as a function of the NH_3 concentration for **1**/LuPc₂ heterojunction devices, at 40% and 60% RH, as depicted from Figure S2 and Figure 9.

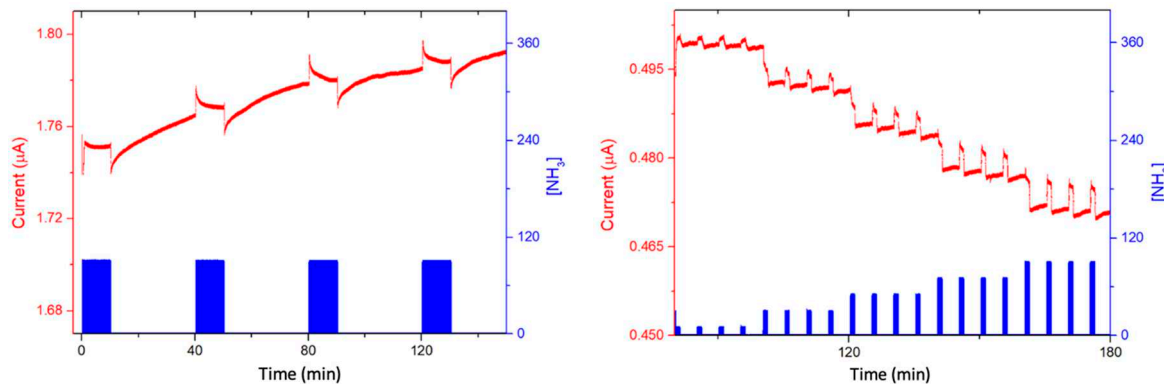


Figure 9. Current variation as a function of time of **1**/LuPc₂ heterojunction exposed to 90 ppm NH_3 for 10 min-long periods separated by 30 min-long rest periods in synthetic air, at 40% RH (left), and in the range 10-90 ppm with 1 min/4 min exposure/recovery cycles at 60% RH (right), both at a bias of 3 V.

For **1**/LuPc₂ heterojunction, long exposure to ammonia highlighted a sharp increase of current under NH_3 as happens for n-type materials, indicating that the majority charge carriers are electrons. However, the sharp increase was followed by a slow decrease during exposure, then, during recovery, a sharp decrease followed by a slow increase were observed (Figure 9 left). During short exposure/recovery cycles the trends remained the same, i.e. sharp current increase and decrease were observed at the beginning of new exposure and recovery periods, respectively (Figure S2). However, as the exposure time is shorter the current decrease during the total exposure period is negligible compared to the short time variations. More interesting, the sharp current variations increase with the NH_3 concentration, the absolute response (ΔI) and relative response (RR) increasing linearly between 10 and 70 ppm (Figure 8 right). The mean sensitivity value for all the concentration range was ca. 0.6 % ppm⁻¹.

For a better understanding of this behavior, we have submitted for 2 h the device to a 500 ml min⁻¹ flow of synthetic air at 60% RH. Then, we performed the same short exposure/recovery cycles in the range 10-90 ppm NH_3 , at 60% RH (Figure 9 right). It shows the same trend observed at 40% RH, but with an increase of current which seems to be higher with the increase of RH. In that case, the absolute response (ΔI) and relative response (RR) increase linearly with the NH_3 concentration in all the studied range (10-90 ppm) (Figure 8 right) and the sensitivity is 0.9% ppm⁻¹. Clearly, the sensitivity increases with the RH value, even though the ΔI value is quasi unchanged in both experiments.

We confirmed this dependence of the response to NH_3 on the RH value by performing experiments at a fixed NH_3 value (50 ppm) in the range 30-60% RH, with short exposure/recovery cycles (Figure S3). Whatever the RH value, the current increases, indicating that the majority free charge carriers remain n-type, contrarily to what we previously observed with ambipolar sublayers [22,34].

The difference in the nature of majority charge carriers between the two devices can be correlated with the frontier energy levels of the two corrole complexes. Due to the presence of pentafluorophenyl moieties, corrole **1** is easier to reduce and more difficult to oxidize, correlated to a stabilization of its HOMO and LUMO orbitals, compared to $\text{Cu}(\text{p-methoxy})\text{TPC}$, by ca. 0.5 eV, as depicted from the present electrochemical study. As a result, it is easier to inject electrons from electrodes towards the fluorinated corrole material.

3.4. Humidity sensing properties

The response of the devices toward humidity was also studied by steps of 10 min, from 30% to 60% RH. This humidity range was chosen because, in most of the practical applications such as in industries or air quality stations, gas sensors operate within this humidity range. For both devices, the current increases sharply at each 10% RH value increase, and decreases sharply at each 10% RH decrease. The recovery is very good for **1**/LuPc₂ (Figure 10) and total for **2**/LuPc₂ (Figure 11). The current value increases by 6.2% and 7.5% when the RH increases from 30 to 60% for **1**/LuPc₂ and **2**/LuPc₂, respectively. The former exhibits an hysteresis, the current remaining higher when RH value decreases (Figure 10 right). The current variation as a function of the RH value is almost linear, with a linear fit leading to a R^2 coefficient of 0.98. for increasing and decreasing RH values. For the latter, only a small difference appears for the current between increasing and decreasing RH values (Figure 11 right).

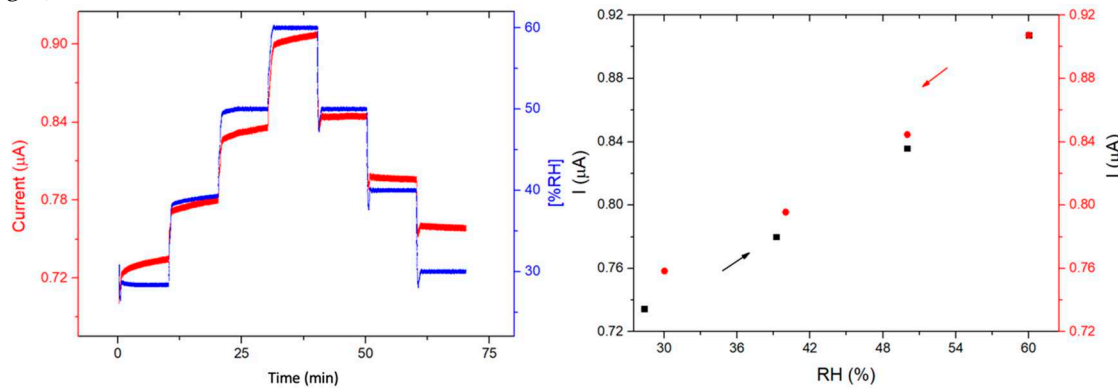


Figure 10. Response of **1**/LuPc₂ heterojunction device to humidity as a function of time (left) and current values as a function of RH (right), with a bias of 1 V.

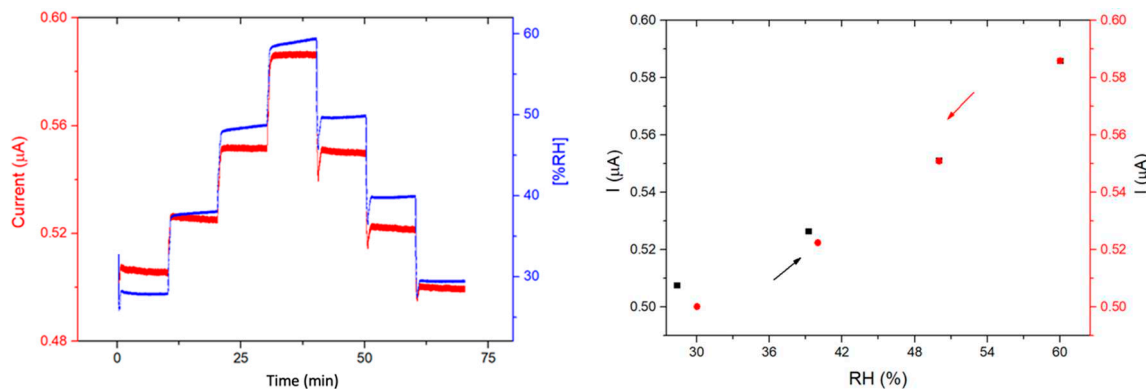


Figure 11. Response of 2/LuPc₂ heterojunction device to humidity as a function of time (left) and current values as a function of RH (right), with a bias of 1 V.

4. Conclusion

Two types of heterojunction devices with two different corroles complexes, namely Cu(III)-tris (pentaFphenyl) corrole and Cu(III)-tris (p-methoxyphenyl) corrole have been developed, by combination with an intrinsic molecular semiconductor, the lutetium bisphthalocyanine. The devices have been characterized by optical measurements such as UV-visible and Raman spectroscopies. About the sensing properties, both devices showed a different behavior towards ammonia. The one with the Cu(III)-tris (p-methoxyphenyl) corrole complex exhibits current decreases under ammonia, showing its p-type behavior. In the case of Cu(III)-tris (pentaFphenyl) corrole complex, current increases under ammonia, showing its n-type behavior. This difference can be correlated with the frontier energy levels of the two corroles complexes. Due to the presence of pentafluorophenyl moieties, the Cu(pentaF)TPC is easier to reduce and more difficult to oxidize, correlated to a stabilization of its HOMO and LUMO orbitals, compared to Cu(p-methoxy)TPC. In addition, both materials show a high sensitivity to humidity, but with a complete reversibility, which is rarely observed in conductometric sensors.

Author Contributions: The idea of the research work was proposed by M.B., C.D.N. and R.P. Experiments were achieved by L.D.Z., with the help of R.P. for the synthesis of corroles, of S.G.M. for the electrical measurements and of R.M.P. for the electrochemical study. The first draft of the manuscript was written by L.D.Z. and M.B. The manuscript was later edited and corrected by all the authors. The project administration and funding acquisition relevant for the manuscript preparation was performed by M.B., C.D.N. and R.P. All authors have read and agreed to the published version of the manuscript.

Funding: This research received no external funding.

Acknowledgments: The authors acknowledge the Conseil Régional de Bourgogne through the CPER program. This work was also partly supported by the Conseil régional Bourgogne Franche-Comté through the Envergure Program MatElectroCap (2020-2024). The Italian Ministry of Education, University and Research (MIUR) is thanked for the PRIN project SUNSET (R. P., Grant 2017EKCS35_002). The authors thank the Plateforme d'Analyses Chimiques et de Synthèse Moléculaire de l'Université de Bourgogne (PACSMUB) and the SATT Sayens for technical support in the Raman analyses.

Conflicts of Interest: The authors declare no conflict of interest.

References

1. Rakow, N. A.; Suslick, K. S. A colorimetric sensor array for odour visualization. *Nature* **2000**, *406*, 710–713.
2. Bouvet, M.; Pauly, A. Molecular semiconductor-based gas sensors. In *The Encyclopedia of Sensors*; Grimes, C. A.; Dickey, E. C.; Pishko, V., Eds.; American Scientific Publishers, 2006; Vol. 6, pp. 227–270.
3. Paolesse, R.; Monti, D.; Nardis, S.; Di Natale, C. 54 Porphyrin-Based Chemical Sensors. In *Handbook of Porphyrin Science (Volume 12)*; With Applications to Chemistry, Physics, Materials Science, Engineering, Biology and Medicine; World Scientific Publishing Company, 2012; Vol. 15, pp. 121–225.
4. Paolesse, R.; Nardis, S.; Monti, D.; Stefanelli, M.; Di Natale, C. Porphyrinoids for Chemical Sensor Applications. *Chem. Rev.* **2017**, *117*, 2517–2583.
5. Parra, V.; Rei Vilar, M.; Battaglini, N.; Ferraria, A. M.; Botelho do Rego, A. M.; Boufi, S.; Rodríguez-Méndez, M. L.; Fonavas, E.; Muzikante, I.; Bouvet, M. New Hybrid Films Based on Cellulose and Hydroxygallium Phthalocyanine. Synergetic Effects in the Structure and Properties. *Langmuir* **2007**, *23*, 3712–3722.
6. Di Natale, C.; Filippini, D.; Pennazza, G.; Santonico, M.; Paolesse, R.; Bellincontro, A.; Mencarelli, F.; D'Amico, A.; Lundström, I. Sorting of apricots with computer screen photoassisted spectral reflectance analysis and electronic nose. *Sens. Actuators: B. Chem.* **2006**, *119*, 70–77.
7. Cetó, X.; Apetrei, C.; del Valle, M.; Rodríguez-Méndez, M. L. Evaluation of red wines antioxidant capacity by means of a voltammetric e-tongue with an optimized sensor array. *Electrochim. Acta* **2014**, *120*, 180–186.
8. Di Natale, C.; Macagnano, A.; Martinelli, E.; Paolesse, R.; D'Arcangelo, G.; Roscioni, C.; Finazzi-Agrò, A.; D'Amico, A. Lung cancer identification by the analysis of breath by means of an array of non-selective gas sensors. *Biosensors and Bioelectronic* **2003**, *18*, 1209–1218.

9. Barbe, J.-M.; Canard, G.; Brandès, S.; Guilard, R. Organic-Inorganic Hybrid Sol-Gel Materials Incorporating Functionalized Cobalt(III) Corroles for the Selective Detection of CO. *Angew. Chem. Int. Ed.* **2005**, *44*, 3103–3106.
10. Wang, Y.; Akhigbe, J.; Ding, Y.; Brückner, C.; Lei, Y. meso-Tritolylcorrole-Functionalized Single-walled Carbon Nanotube Donor-Acceptor Nanocomposites for NO₂ Detection. *Electroanalysis* **2012**, *24*, 1348–1355.
11. Santos, C. I. M.; Oliveira, E.; Barata, J. F. B.; Faustino, M. A. F.; Cavaleiro, J. A. S.; Neves, M. G. P. M. S.; Lodeiro, C. Corroles as anion chemosensors: exploiting their fluorescence behaviour from solution to solid-supported devices. *J. Mater. Chem.* **2012**, *22*, 13811–13819.
12. Vanotti, M.; Poisson, S.; Soumann, V.; Quesneau, V.; Brandès, S.; Desbois, N.; Yang, J.; André, L.; Gros, C. P.; Blondeau-Patissier, V. Influence of interfering gases on a carbon monoxide differential sensor based on SAW devices functionalized with cobalt and copper corroles. *Sens. Actuators: B. Chem.* **2021**, *332*, 129507.
13. Di Natale, C.; Gros, C. P.; Paolesse, R. Corroles at work: a small macrocycle for great applications. *Chem. Soc. Rev.* **2022**, *51*, 1277–1335.
14. Johnson, A. W.; Kay, I. T. 306. Corroles. Part I. Synthesis. *J. Chem. Soc.* **1965**, 1620–1629.
15. Paolesse, R.; Mini, S.; Sagone, F.; Boschi, T.; Jaquinod, L.; Nurco, D. J.; Smith, K. M. 5,10,15-Triphenylcorrole: a product from a modified Rothemund reaction. *Chem. Commun.* **1999**, 1307–1308.
16. Gross, Z.; Galili, N.; Saltsman, I. The First Direct Synthesis of Corroles from Pyrrole. *Angew. Chem. Int. Ed. Engl.* **1999**, *38*, 1427–1429.
17. Tang, J.; Chen, B.; Zhang, Y.; Lu, J.; Zhang, T.; Guo, Q.; Zhang, J. Synthesis and gas sensitivity properties of novel metallocorroles and functionalized graphene oxide. *Function. Mater. Lett.* **2019**, *12*, 1940001.
18. Parra, V.; Brunet, J.; Pauly, A.; Bouvet, M. Molecular semiconductor-doped insulator (MSDI) heterojunctions: an alternative transducer for gas chemosensing. *Analyst* **2009**, *134*, 1776–1778.
19. Mateos, M.; Meunier-Prest, R.; Heintz, O.; Herbst, F.; Suisse, J.-M.; Bouvet, M. Comprehensive Study of Poly(2,3,5,6-tetrafluoroaniline): From Electrosynthesis to Heterojunctions and Ammonia Sensing. *ACS Appl. Mater. Interfaces* **2018**, *10*, 19974–19986.
20. Kumar, A.; Alami Mejjati, N.; Meunier-Prest, R.; Krystianik, A.; Heintz, O.; Lesnewska, E.; Devillers, C. H.; Bouvet, M. Tuning of interfacial charge transport in polyporphine/phthalocyanine heterojunctions by molecular geometry control for an efficient gas sensor. *Chem. Eng. J.* **2022**, *429*, 132453.
21. Di Zazzo, L.; Kumar, A.; Meunier-Prest, R.; Di Natale, C.; Paolesse, R.; Bouvet, M. Electrosynthesized copper polycorroles as versatile materials in double lateral heterojunctions. *Chem. Eng. J.* **2023**, *458*, 141465.
22. Ouedraogo, S.; Meunier-Prest, R.; Kumar, A.; Bayo-Bangoura, M.; Bouvet, M. Modulating the Electrical Properties of Organic Heterojunction Devices Based On Phthalocyanines for Ambipolar Sensors. *ACS Sens.* **2020**, *5*, 1849–1857.
23. Wannebroucq, A.; Gruntz, G.; Suisse, J.-M.; Nicolas, Y.; Meunier-Prest, R.; Mateos, M.; Tourance, T.; Bouvet, M. New n-type molecular semiconductor-doped insulator (MSDI) heterojunctions combining a triphenodioxazine (TPDO) and the lutetium bisphthalocyanine (LuPc₂) for ammonia sensing. *Sens. Actuators: B. Chem.* **2018**, *255*, 1694–1700.
24. Sahin, Z.; Meunier-Prest, R.; Dumoulin, F.; Kumar, A.; Isci, U.; Bouvet, M. Tuning of organic heterojunction conductivity by the substituents' electronic effects in phthalocyanines for ambipolar gas sensors. *Sens. Actuators: B. Chem.* **2021**, *332*, 129505.
25. Bouvet, M. Radical phthalocyanines and intrinsic semiconduction. In *The Porphyrin Handbook*; Kadish, K. M.; Smith, K. M.; Guilard, R., Eds.; Academic Press: Amsterdam, 2003; Vol. 19, pp. 37–103.
26. Bouvet, M.; Ouedraogo, S.; Meunier-Prest, R. Ambipolar materials for gas sensors. In *Ambipolar materials and devices*; Zhou, Y.; Han, S. T., Eds.; Royal Society of Chemistry, Chap.16, 2020.
27. Clarisse, C.; Riou, M. T. Synthesis and characterization of some lanthanide phthalocyanines. *Inorg. Chim. Acta* **1987**, *130*, 139–144.
28. Paolesse, R.; Nardis, S.; Sagone, F.; Khouri, R. G. Synthesis and Functionalization of meso-Aryl-Substituted Corroles. *J. Org. Chem.* **2001**, *66*, 550–556.
29. Bouvet, M.; Xiong, H.; Parra, V. Molecular semiconductor-doped insulator (MSDI) heterojunctions: Oligothiophene/bisphthalocyanine (LuPc₂) and perylene/bisphthalocyanine as new structures for gas sensing. *Sens. Actuators: B. Chem.* **2010**, *145*, 501–506.
30. Ahmida, M. M.; Eichhorn, S. H. Measurements and prediction of electronic properties of discotic liquid crystalline triphenylenes and phthalocyanines. *ECS Transactions*, 2010; Vol. 25, pp. 1–10.

31. Chen, Y.; Bouvet, M.; Sizun, T.; Gao, Y.; Plassard, C.; Lesniewska, E.; Jiang, J. Facile approaches to build ordered amphiphilic tris(phthalocyaninato) europium triple-decker complex thin films and their comparative performances in ozone sensing. *Phys. Chem. Chem. Phys.* **2010**, *12*, 12851–11.
32. Bouvet, M.; Parra, V.; Suisse, J. M. Molecular semiconductor-doped insulator (MSDI) heterojunctions as new transducers for chemical sensors. *Eur. Phys. J. Appl. Phys.* **2011**, *56*, 34103–10.
33. Wasbotten, I. H.; Wondimagegn, T.; Ghosh, A. Electronic Absorption, Resonance Raman, and Electrochemical Studies of Planar and Saddled Copper(III) meso-Triarylcorroles. Highly Substituent-Sensitive Soret Bands as a Distinctive Feature of High-Valent Transition Metal Corroles. *J. Am. Chem. Soc.* **2002**, *124*, 8104–8116.
34. Wannebroucq, A.; Ouedraogo, S.; Meunier-Prest, R.; Suisse, J.-M.; Bayo, M.; Bouvet, M. On the interest of ambipolar materials for gas sensing. *Sens. Actuators: B. Chem.* **2018**, *258*, 657–664.

Disclaimer/Publisher's Note: The statements, opinions and data contained in all publications are solely those of the individual author(s) and contributor(s) and not of MDPI and/or the editor(s). MDPI and/or the editor(s) disclaim responsibility for any injury to people or property resulting from any ideas, methods, instructions or products referred to in the content.